Geological Survey of Japan Cruise Report No. 23, p. 201-207, 1994

XI. HEAT FLOW IN THE PENRHYN BASIN, SOUTH PACIFIC (GH83-3 AREA)

Toshitsugu Yamazaki

Introduction

Heat flow measurements were carried out in the Penrhyn Basin, a Mesozoic seafloor to the east of the Manihiki Plateau in the south Pacific during the GH83-3 cruise of the R/V Hakurei-maru as part of the research program, "Geological Study of Deep-Sea Mineral Resources." The purpose of the measurement is to collect basic data for understanding better the geological history of this area and its relation to formation of manganese nodules. Few heat flow data were previously reported in this area (Matsubayashi, 1982).

In this report, I present eleven new heat flow data in the Penrhyn Basin. The heat flow data and seafloor depth are compared with those of the theoretical prediction based on a plate cooling model. I discuss the age and thermal history of the seafloor of the study area.

Geological Setting

The Penrhyn Basin is located off the eastern margin of the Manihiki Plateau (Fig. XI-1). The Manihiki Plateau is one of midplate swells in the Pacific, and was dated as 123±1.5 Ma by the ^{40}Ar-^{39}Ar method (Mahoney *et al.*, 1993). No magnetic lineation has been found in the Penrhyn Basin (Golovchenko *et al.*, 1981; Yamazaki and Okuda, Chapter XIII of this volume). On the other hand, magnetic lineations of north-south direction produced by Cenozoic seafloor spreading at the East Pacific Rise occur to the east of the Penrhyn Basin (e.g. Mayes *et al.*, 1990). It is thus considered that the Penrhyn Basin belongs to the Cretaceous Magnetic Quiet Zone (83- 124 Ma; Harland *et al.*, 1990). Tectonic reconstruction by Joseph *et al.* (1993) suggests that the Penrhyn Basin was produced by Pacific-Farallon spreading of NNW- SSE direction after the reorganization of spreading system at M0 time (124 Ma).

To the southeast of the Penrhyn Basin, hotspot-origin volcanic islands of the French Polynesia are distributed (Fig. XI-1). This is an anomalously shallow and hot region called the South Pacific Superswell (McNutt and Fischer, 1987). It is proposed that a large mantle plume rises from the core-mantle boundary beneath this region (Fukao, 1992).

The study area (GH83-3 area) is in the southwestern part of the Penrhyn Basin. Detailed topography of this area has not yet been clarified except for the detailed

Keywords: heat flow, Cretaceous, pelagic clay, hot spot, Manihiki Plateau, Hakurei-Maru, Penrhyn Basin

survey area (a box in Fig. XI-1). Water depth of the study area excluding small seamounts ranges mostly from 5200 to 5300 m. Exceptions are a conspicuous trough and ridge system striking NNW-SSE. The maximum water depth of the trough reaches 6000 m. The strike of the trough-ridge system, which is close to that of the Pacific-Farallon spreading, suggests its paleo-rift origin.

Surface sediments of the GH83-3 area are composed of pelagic clay (red clay), and

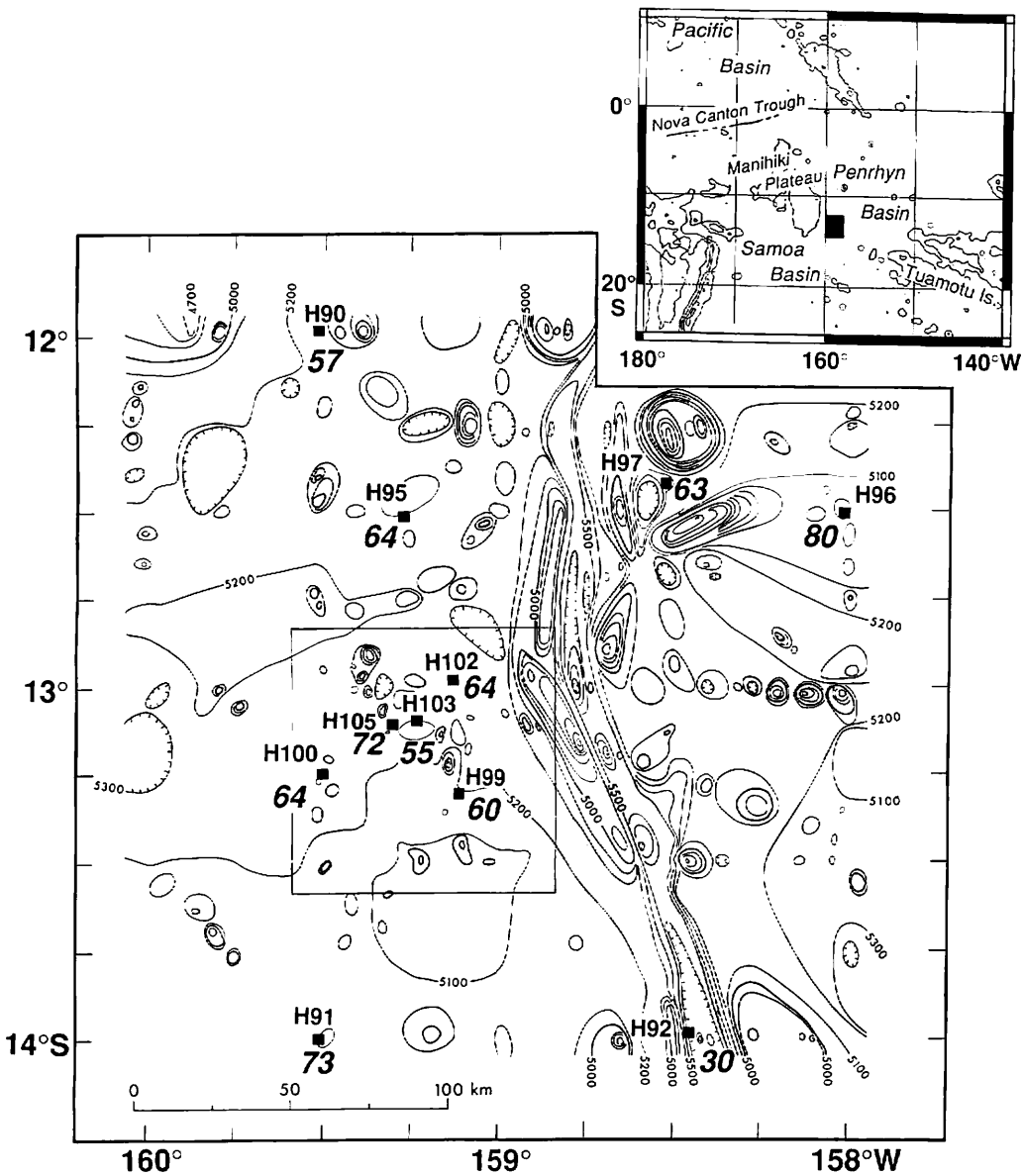

Fig. XI-1 Topography and heat flow (mW/m²) in the GH83-3 area. A box is the detailed survey area.

completely devoid of siliceous or calcareous microfossils. This is because water depth of the study area is below the Carbonate Compensation Depth, which is about 4500 m at present (Berger and Winterer, 1974), and the area is off the biological high-productivity zone along the equator. The surface sediments can be classified as Units I , II and III based on records of 3.5 kHz subbottom profiler and lithology of cored sediments (Nishimura and Saito, Chapter IV in this volume). Unit I is unconsolidated pelagic clay of Miocene or younger, and Units II and III is semi-consolidated pelagic clay of Eocene or older. A remarkable hiatus with manganese crust occurs between Unit I and II. Some places has thin or almost no Unit I sediments because of extremely slow sedimentation or erosion due to intense bottom current.

Measurements

Most of the measurements were carried out on flat floors of the basin at depths ranging from 5200 to 5300 m (Fig. XI-1). Exceptions are H92 and H96. The former is on an abyssal hill, and the latter is on the bottom of the NNW-trending trough.

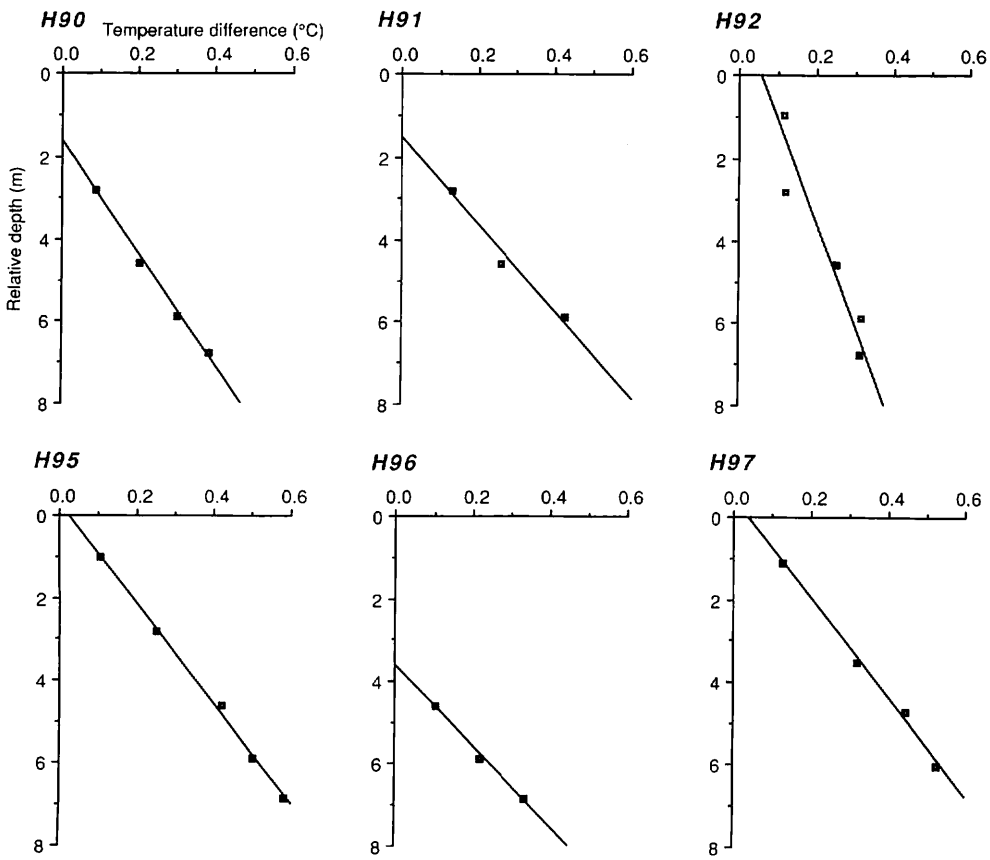

Fig. XI-2 Sediment temperature profiles for successful penetrations. Vertical axis represents the length of a probe (core barrel). Horizontal axis represents difference from the temperature of bottom water just above the seafloor of each site. Thermal gradient was calculated by fitting a straight line using a least squares method.

Thermal gradient

Two units of GH80-1 type thermograd-meter (Matsubayashi, 1982), which has three thermistors each, were used simultaneously at each measurement. A pair of thermistors (one for each apparatus) was attached at the same position to calibrate the two apparatus. Thus temperatures at five different depths in sediments can be obtained in case of full penetration. Temperature data were digitized every 60 seconds. Thermistors were mounted at 1 to 1.5 m intervals on an 8-m (or 4-m) core barrel like an outrigger. Temperature of each thermistor in sediments was measured relative to bottom-water temperature obtained at about 30 m above the seafloor immediately after pulling out from the sediments.

Decay of frictional heating of the thermistors during penetration into sediments was monitored for 12 minutes. Equilibrium temperature of each thermistor was obtained by the extrapolation using cylindrical decay function $F(\alpha,\tau)$ of Bullard (1954). I used a simple linear fit to the $F(\alpha,\tau)$ vs. temperature plot. The decay origin time was adjusted by trial and error to get linear $F(\alpha,\tau)$ decay (Villinger and Davis, 1987). Thermal disturbances due to the movement of the probe during the frictional decay monitoring cause non-linear, anomalous $F(\alpha,\tau)$ decay plots, and these measurements were discarded. Penetrating into soft sediments of Unit I produced little frictional

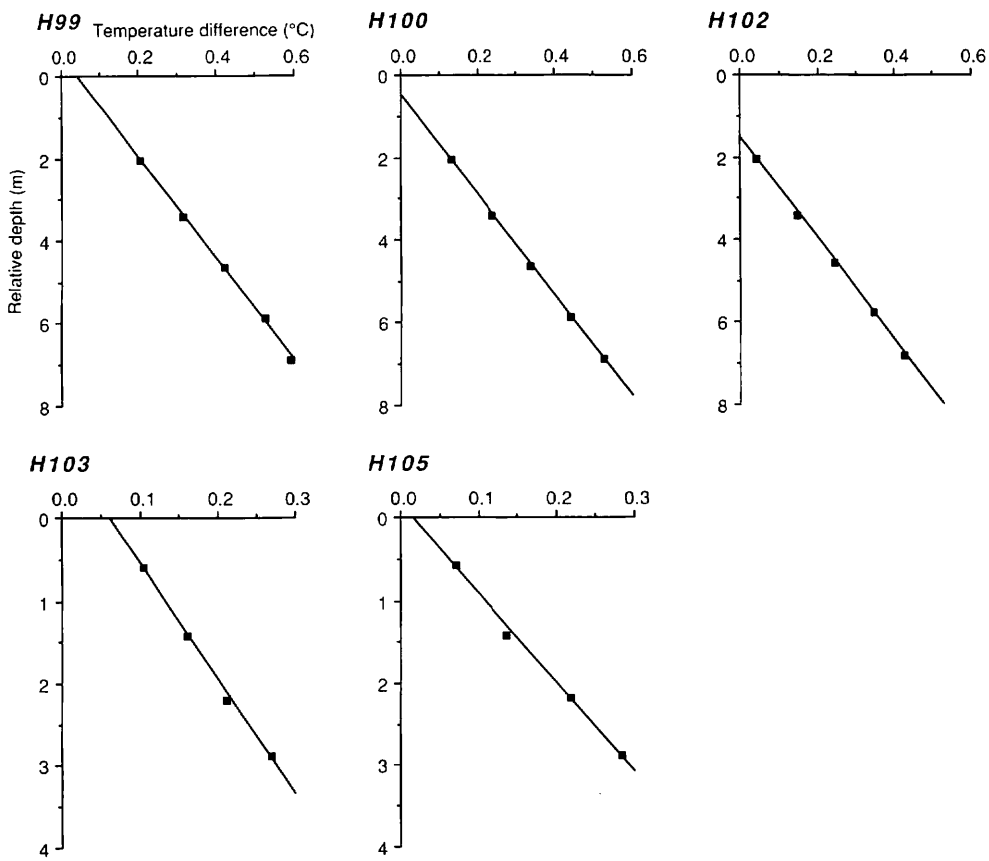

Fig. XI-2 (continued)

heating, and the extrapolated temperatures of these sites (H90, H92, H95, H97, H99, H100, H102 and H103) have negligible error less than 0.01°C. However, semi-consolidated sediments of Unit II and III caused large friction against the penetration. The corer sometimes fell down on hitting the seafloor or before completion of frictional decay monitoring. Even in the case of successful penetration, large frictional heat may have caused a large error in the extrapolated equilibrium temperature (H91, H96 and H105).

An average thermal gradient was calculated by fitting a straight line on depth-temperature plots using the least-squares method (Fig. XI-2). Linearity of thermal gradient is good except for H91 and H92. The absolute depth of each thermistor in sediments is unknown due to difficulty in measuring accurate penetration depth of a corer. The figure is drawn assuming full penetration of core barrel.

Thermal conductivity

Thermal conductivity of half-split cores was measured using QTM (Quick Thermal conductivity Meter, manufactured by Showa Denko Co.) at intervals of 30 to 50 cm. The QTM was calibrated using standards of fused quartz and acrylic resin (manufacture's recommended values are 1.39 and 0.241 W/mK, respectively). The accuracy is within ±5% (Sass *et al.*, 1984; Galson *et al.*, 1987). Cores were split into halves immediately after recovery, and covered with thin plastic film to prevent dehydration. Measurements were done on board as soon as the thermal steady state was attained at about 25°C in several hours after recovery. The effect of the plastic film is negligible (Sass *et al.*, 1984).

The simple mean of thermal conductivity values along a core after correction for the effects of in situ temperature and pressure (Ratcliffe, 1960) was used for calculating heat flow (Table XI-1). Variations of the thermal conductivity within and among

Table XI-1 Summary of heat flow measurements.

Station	Latitude (S)	Longitude (W)	Depth (m)	N	G (10^{-2}K/m)	K (W/mK)	Q (mW/m^2)
H90 (P396)	11°58.82'	159°31.06'	5289	4	7.38	0.766±0.013	56.5
H91 (P397)	13°59.77'	159°31.02'	5176	3	9.48	0.773±0.018	73.3
H92 (P398)	13°58.53'	158°27.69'	5727	5	4.01	0.754±0.012	30.2
H95 (P401)	12°30.56'	159°16.00'	5206	5	8.34	0.765±0.028	63.8
H96 (P402)	12°30.25'	158°00.83'	4950	3	10.25	0.778±0.022	79.7
H97 (P403)	12°24.80'	158°31.15'	5330	4	8.38	0.757±0.011	63.4
H99 (P405)	13°17.96'	159°06.51'	5238	5	8.13	0.742±0.018	60.3
H100 (P406)	13°14.66'	159°30.16'	5268	5	8.23	0.775±0.024	63.8
H102 (P408)	12°58.65'	159°07.68'	5258	5	8.16	0.784±0.011	64.0
H103 (P409)	13°05.56'	159°14.06'	5186	5	7.15	0.765±0.016	54.7
H105 (P411)	13°06.16'	159°18.01'	5217	4	9.38	0.771±0.020	72.3

N : Number of active thermistors in sediments.
G : Thermal gradient.
K : Thermal conductivity.
Q : Heat flow.

cores are small (Table XI-1), which reflects relatively uniform composition of the sediments.

Results and Discussion

The results of eleven successful heat flow measurements out of seventeen trials are summarized in Table XI-1. Simple mean and standard deviation of the eleven heat flow values are 62.0 ± 12.3 mW/m^2. Site H92, which is located at the bottom of the trough, shows anomalously low heat flow (30 mW/m^2) with poor linearity of temperature gradient (Fig. XI-2). The low value may be caused by pore water advection through fault scarps bounding the trough, which would have thin or no sediment cover. Quality of temperature gradient data of H91, H96 and H105 is lower than other sites because of large frictional heating as mentioned above. If these four sites are excluded, the mean and standard deviation of the seven data of higher quality are 60.9 ± 3.6 mW/m^2.

Stein and Stein (1992) has recently proposed a new model (GDH1) for the age-dependence of heat flow and depth on oceanic lithosphere based on a plate cooling model. This model has a hotter and thinner lithosphere than previous models (e.g. Parsons and Sclater, 1977), and well fits global averages of heat flow and depth. The seafloor in the GH83-3 area is considered to belong to the Cretaceous Magnetic Quiet Zone (CMQZ). The model GDH1 predicts the heat flow of 57.6 mW/m^2 and the depth of 5404 m for the age of 83 Ma, that is, at the end of CMQZ. For the age of 124 Ma (at the beginning of CMQZ), they are 51.0 mW/m^2 and 5572 m, respectively.

The observed heat flow of the GH83-3 area is close to the prediction for 83 Ma, but a little higher than that for 124 Ma. Average water depth of the seafloor in the study area is about 5250 m except for the trough and seamounts. In this region, sediment thickness covering the basement ranges from 0.2 to 0.3 seconds in two-way travel time on seismic reflection profiles (Okuda *et al.*, Chapter II of this volume). Basement depth after the correction of sediment loading (Crough, 1983) is hence estimated to be about 5400 m. Thus the observed basement depth also agree with the prediction for 83 Ma, but is shallower than that for 124 Ma.

The following two possibilities for the thermal history of this area can be derived from these results: (1) the seafloor was formed in the late Cretaceous, and has not been affected by the hot spots at the South Pacific Superswell since then, or (2) the seafloor was created in the middle Cretaceous, and then the lithosphere was somewhat reheated by the activity of the hot spots. To distinguish these two models, it is necessary to obtain and date basalts which consist the basement.

References

Berger, W.H. and Winterer, E.L. (1974) Plate stratigraphy and the fluctuating carbonate line. *Intl. Assoc. Sedimentologists Spec. Pub.*, vol. 1, p. 11-48.

Bullard, E.C. (1954) The flow of heat through the floor of the Atlantic Ocean. *Proc. Roy. Soc. Lond. Ser. A*, vol. 222, p. 408-429.

Crough, S.T. (1983) The correction for sediment loading on the seafloor. *J. Geophys. Res.*, vol. 88, p. 6449-6454.

Fukao, Y. (1992) Seismic tomography of the Earth's mantle: geodynamic implications. *Science*, vol. 258, p. 625-630.

Galson, D.A., Wilson, N.P., Schärli, U. and Rybach, L. (1987) A comparison of the divided-bar and QTM methods of measuring thermal conductivity. *Geothermics*, vol. 16, p. 215-226.

Golovchenko, X., Larson, R.L. and Pitman III, W.C. (1981) *Plate-tectonic map of the circum-Pacific region, Southwest quadrant, magnetic lineations.* Amer. Assoc. Petrol. Geol., Tulsa.

Harland, W.B., Armstrong, R.L., Cox, A.V., Craig, L.E., Smith, A.G. and Smith, D. G. (1990) *A Geologic Tme Scale 1989.* Cambridge University Press, Cambridge, 263pp.

Joseph, D., Taylor, B., Shor, A.N. and Yamazaki, T. (1993) The Nova-Canton Trough and the Late Cretaceous evolution of the Central Pacific. In: Pringle, M. *et al.* (eds.), *The Mesozoic Pacific,* AGU Monograph, vol. 77, p. 171-185.

Mahoney, J.J., Storey, M., Duncan, R.A., Spencer, K.J. and Pringle, M. (1993) Geochemistry and age of the Ontong-Java Plateau. In: Pringle, M. *et al.* (eds.), *The Mesozoic Pacific,* AGU Monograph, vol. 77, p. 233-261.

Matsubayashi, O. (1982) Reconnaissance measurements of heat flow in the Central Pacific. *Geol. Surv. Japan Cruise Rept.*, no. 18, p. 90-94.

Mayes, C.L., Lawver, L.A. and Sandwell, D.T. (1990) Tectonic history and new isochron chart of the South Pacific. *J. Geophys. Res.*, vol. 95, p. 8543-8567.

McNutt, M.K. and Fischer, K.M. (1987) The South Pacific Superswell. In: Keating, B.H. *et al.* (eds.), *Seamounts, Islands, and Atolls.* AGU Monograph, vol. 43, Amer. Geophys. Union, Washington, D.C., p. 25-34.

Parsons, B. and Sclater, J.G. (1977) An analysis of the variation of ocean floor bathymetry and heat flow with age. *J. Geophys. Res.*, vol. 82, p. 803-827.

Ratcliffe, E.H. (1960) The thermal conductivities of ocean sediments. *J. Geophys. Res.*, vol. 65, p. 1535-1541.

Sass, J.H., Stone, C. and Munroe, R.J. (1984) Thermal conductivity determinations on solid rock - a comparison between a steady-state divided-bar apparatus and a commercial transient line-source device. *J. Volcanol. Geotherm. Res.*, vol. 20, p. 145-153.

Stein, C.A. and Stein, S. (1992) A model for the global variation in oceanic depth and heat flow with lithospheric age. *Nature*, vol. 359, p. 123-129.

Villinger, H. and Davis, E.E. (1987) A new reduction algorithm for marine heat flow measurements. *J. Geophys. Res.*, vol. 92, p. 12846-12856.